arXiv:1601.03784v1 [cond-mat.dis-nn] 15 Jan 2016

Localization of weakly disordered flat band states

Daniel Leykam,[1,2] Joshua D. Bodyfelt,[3] Anton S. Desyatnikov,[1,4] and Sergej Flach[3,5]

[1] *Nonlinear Physics Centre, Research School of Physics and Engineering, The Australian National University, Canberra ACT 2601, Australia*

[2] *Division of Physics and Applied Physics, School of Physical and Mathematical Sciences, Nanyang Technological University, Singapore 637371, Singapore*

[3] *New Zealand Institute for Advanced Study, Centre for Theoretical Chemistry & Physics, Massey University, 0745 Auckland, New Zealand*

[4] *Physics Department, School of Science and Technology, Nazarbayev University, 53 Kabanbay Batyr Ave., Astana, Kazakhstan*

[5] *Center for Theoretical Physics of Complex Systems, Institute for Basic Science, Daejeon, Korea*

(Dated: January 18, 2016)

Certain tight binding lattices host macroscopically degenerate flat spectral bands. Their origin is rooted in local symmetries of the lattice, with destructive interference leading to the existence of compact localized eigenstates. A recent study of a particular one-dimensional lattice [EPL **105**, 30001 (2014)] showed that weak diagonal disorder hybridizes compact eigenstates with dispersive bands, leading to Fano resonances, Cauchy-tailed effective disorder potentials, and a loss of single parameter scaling. Here we generalize to different classes of flat band lattices in one and two dimensions as well as off-diagonal disorder, revealing different scaling exponents for the Anderson localization length and confirming the broad applicability of the underlying Fano-Cauchy physics.

PACS numbers: 03.65.Ge, 73.20.Fz

I. INTRODUCTION

Wave dynamics reflect the symmetries and topologies imprinted by an underlying periodic potential. Restrictions to a few bands of the dispersion relation lead to effective lattice equations. The resulting wave nature, *i.e.* the corresponding characteristic lengths and time scales, can vary strongly. Examples include electrons in crystals or in artificial quantum dot arrays [1], ultracold atoms in optical lattices [2], microwaves in dielectric resonator networks [3], and light propagation in waveguide networks [4]. The width of one of these bands corresponds to a certain amount of available kinetic energy. Additional interactions between the constituent waves lead to interesting new phenomena under competition with the kinetic energy (for instance, see references in recent reviews on topological flat bands [5, 6]). The more narrow the band, the weaker the interaction strength needed to get into nonperturbative interaction regimes.

A particularly interesting situation arises when some of the dispersion parts become strictly *flat*. Such flat bands (FB) have been studied in a number of lattice models in three-dimensional, two-dimensional, and even one-dimensional (1D) settings [7–9], and recently realized experimentally with photonic waveguide arrays [10–12], exciton-polariton condensates [13, 14], and cold atoms [15]. In this case, any *relevant* perturbation may lift the macroscopic degeneracy, and define the type of emerging eigenstates. Most of the lattice models with flat bands are obtained by intuitive procedures, leaving open questions. Is there a constructive way to generate flat band models? Can such a construction method help in detangling flat band (FB) states from the dispersive part of the lattice? Can this be used to track the impact of a perturbation in a systematic way? An especially relevant perturbation is disorder, which is inevitable in any physical system. Anderson localization in these flat band systems is thus an interesting problem, which has been explored in several recent works [16–20].

Several FB construction pathways using graph theory were suggested [7, 21–24]. Another route uses compact eigenstates which are fully localized on several lattice sites [7, 25]. The origin of such a compact localized state (CLS) is destructive interference, effectively decoupling it from the rest of the lattice. A recently published detangling procedure allows to transform FB models hosting CLS into Fano lattices [26], whereby a perturbative diagonal disorder potential is split into two parts. With the use of the local symmetries of a CLS, the first part lifts their degeneracy, while keeping the eigenstates compact. The second perturbative part hybridizes the CLS with the continuum of dispersive degrees of freedom, in analogy with Fano resonances [27]. The result for a particular 1D cross-stitch network was the localization length ξ scaling with diagonal disorder strength W as $\xi \sim 1/W$ at the FB energy – at variance to the familiar $\xi \sim 1/W^2$ law away from the FB energy [26].

In this work, we apply the detangling ideas [26] to a variety of different quasi-1D and 2D lattices, and consider both diagonal and off-diagonal disorder. We find that in all cases, weak disorder turns a CLS into a strong Fano scatterer for dispersive waves under an effective Cauchy-tailed disorder. We characterize disordered FB states by computing how their localization length scales with weak disorder, displaying a whole variety of unconventional emerging exponents and a violation of single parameter scaling [28, 29], confirming the broad applicability of the Fano-Cauchy physics. We show that in 2D

lattices Fano scatterers can no longer trap and localize waves, but resonances still affect the scaling of other measures of localization such as the eigenmode participation number.

We start by reviewing the detangling procedure for flat band lattices in Sec. II and Anderson localization under the resulting Cauchy-tailed disorder in Sec. III, before applying the detangling to four 1D example lattices in Sec. IV. Sec. V discusses the generalization to 2D systems and we summarize our results in Sec. VI.

II. FLAT BAND MODELS, COMPACT LOCALIZED STATES, AND DETANGLING

Consider a lattice wave eigenvalue problem of the type $E\Psi_n = \epsilon_n \Psi_n - \sum_m t_{nm}\Psi_m$, where the wave components Ψ_n are complex scalars allocated to points on a periodic lattice, the matrix t_{nm} defines an interaction between them, and ϵ_n are onsite energies. The eigenvectors of such a tight binding model are delocalized Bloch waves with eigenenergies $E_\nu(\vec{k})$ forming a band structure, where $\vec{k}$ is the Bloch wavevector and $\nu = 1, ..., \mu$ is the band index. Excluding the trivial case of just one band, $\mu = 1$, we consider models with at least one FB for which $E_\nu(\vec{k}) = const.$ Due to the macroscopic degeneracy of the FB, its Bloch waves may be mixed to obtain localized FB eigenvectors (analogous to the construction of Wannier functions [30]). It is tempting to search for cases supporting *compact* localized eigenvectors that are strictly zero outside a finite interval [7], although no general theorem guarantees their existence. When they do exist, such compact localized states can be further classified by the number of unit cells they span, U.

The nonzero amplitudes Ψ_n of each CLS define a direction in the vector space formed by the lattice wave amplitudes. A rotation $\hat{D}$ can thus be performed to produce a new basis vector $\vec{e}_{\rm CLS}$ aligning with the CLS direction, along with a remaining set of orthogonal basis vectors $\vec{e}_\perp$. This local rotation, which respects the symmetry of a given CLS, literally rotates the CLS degree of freedom out of the lattice, as illustrated in Fig. 1.

When starting with a network of M lattice points and $N < M$ unit cells, applying this transformation will produce one detangled CLS satisfying a trivial equation of the type $E\Psi_{\mathcal{S}} = E_{FB}\Psi_{\mathcal{S}}$ and $M - 1$ equations for the remaining network. The benefit of applying such a transformation is that perturbations to the original Hamiltonian network can then be split into a symmetric part which maintains the existence of the CLS, but possibly shifting its energy, and an antisymmetric part that couples it into the remaining degrees of freedom (dispersive band states, and possibly a finite number of neighbouring CLS). In particular, we immediately observe that this antisymmtric coupling is *local* in space due to the compact nature of the CLS.

For $U = 1$ the set of all CLS (note that there is always one CLS per flat band and unit cell) forms an orthonormal complete basis for the flat band. For $U > 1$ the CLS lack orthogonality, but may still form a linearly independent set (apparently for all known 1D cases) which forms a complete basis for the flat band. On the other hand, plenty of 2D examples with $U > 1$ have a set of CLS which is linearly dependent. In that case, the missing states which complete the flat band basis are compact localized lines (CLL) extended in one lattice direction while staying compact in the orthogonal one. They originate from protected touchings of the flat band with the edge of a dispersive band and represent a nontrivial mixture of extended (dispersive) and localized (CLS) states [25].

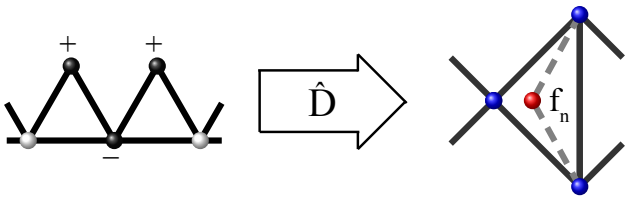

FIG. 1. Schematics of the detangling procedure. Left: the 1D sawtooth lattice. A compact localized state of its flat band excites three sites with amplitudes as indicated by the $\pm$ signs. A local rotation $\hat{D}$ transforms the lattice to its detangled version (right), consisting of decoupled Fano states f_n only coupled to the lattice via perturbations (dashed links), whereas the black links indicate hopping terms (not necessarily uniform) that are nonzero in the absence of perturbations.

For $U = 1$ we can detangle all CLS simultaneously. When $U > 1$, one can perform a similar detangling by considering a superlattice formed by groups of U unit cells. Using such an enlarged unit cell, N/U of the flat band states become CLS of class $U = 1$, which can detangled exactly as above. In many cases this partial detangling of the flat band is sufficient to understand the impact of perturbations such as disorder, especially when the perturbations destroy the translational invariance of the lattice.

III. DISORDER

Now consider the effect of disorder on the above lattices, such that onsite potentials are uncorrelated, uniformly distributed random variables, $\epsilon_n \in [-W/2, W/2]$. Generically, the symmetric part of the disorder will smear out the energy of the CLS to a width W while retaining their compactness. The antisymmetric part couples the CLS to the other dispersive states, which are typically Anderson-localized to a size of $\xi \sim 1/W^2$ [31] in 1D systems, and potentially to neighbouring CLS and to CLL.

We can understand the effect of coupling the disordered CLS to the dispersive states by introducing a generalized Fano-Anderson model [27]. For sufficiently weak disorder, we can restrict our attention to the near-resonant interaction between the CLS and the closest dispersive band. Interaction with other dispersive bands

will be nonresonant and much weaker. In this two-band approximation, the eigenvalue problem reduces to

$$\begin{aligned} Ep_n &= V_n p_n + \epsilon_n^- f_n - p_{n-1} - p_{n+1}, \\ Ef_n &= (E_{FB} + \epsilon_n^+) f_n + \epsilon_n^- p_n, \end{aligned} \tag{1}$$

where p_n are amplitudes corresponding to the nearest dispersive band, f_n are the CLS amplitudes (analogous to Fano states in the Fano-Anderson model), V_n is a bounded term accounting for the effect of disorder on the dispersive band, and $\epsilon_n^{\pm}$ are the (anti)symmetric parts of the disorder potential affecting the FBS. Since the Fano states are locally coupled to the relevant dispersive band, the Fano state amplitudes f_n can be eliminated from Eqs. (1) leaving

$$Ep_n = \left(V_n + \frac{(\epsilon_n^-)^2}{E - E_{FB} - \epsilon_n^+} \right) p_n - p_{n-1} - p_{n+1}. \tag{2}$$

It is immediately seen that the Fano state leads to a resonant enhancement of the effective onsite potential, via the second term in the brackets. In particular, calculating the probability distribution function (PDF) of $z = 1/\epsilon_n^+$ yields [26]

$$\mathcal{W}(z) = \frac{2}{z^2} \int \mathcal{P}(y) \mathcal{P}\left(\frac{2}{z} - y \right) dy,$$

where $\mathcal{P}(x)$ is the PDF of the random variable ϵ_n^+. At $E = E_{FB}$, a bounded uniformly distributed disorder is transformed into one resembling a Cauchy distribution, with heavy tails $\mathcal{W}(z) \sim 1/z^2$ for large z. This type of distribution resembles the Lloyd model [32] – an Anderson-type model in which the onsite energies $\tilde{\epsilon}_n$ are drawn from a Cauchy distribution,

$$\mathcal{P}(x) = \frac{1}{\pi} \frac{W}{x^2 + W^2}.$$

Thouless [33] and Ishii [34] derived the localization length ξ for the Lloyd model, given as

$$4 \cosh(\xi^{-1}) = \sqrt{(2+E)^2 + W^2} + \sqrt{(2-E)^2 + W^2},$$

For energies within the band, $-2 < E < 2$, a Taylor expansion for small ξ^{-1} and W yields

$$\xi^{-1} = W / \sqrt{4 - E^2},$$

Thus, $\xi \sim 1/W^{\nu}$ displays a power law scaling with exponent $\nu = 1$, in contrast to the $\nu = 2$ scaling of the conventional 1D Anderson model.

Similarly, at the dispersive band edge $E = \pm 2$, a weak disorder expansion yields

$$\xi^{-1} = \sqrt{2/W},$$

with exponent $\nu = 1/2$, in contrast to the usual $\nu = 2/3$ when the disorder potential is bounded [35].

In other words, for small W the Lloyd model displays much stronger localization. This can be understood quite simply in terms of the divergent variance of the potential: given a long enough chain, one is certain to encounter a potential barrier large enough to classically trap the wave, *i.e.* larger than the wave's kinetic energy. In contrast, the localization mechanism for small W in the Anderson model is weak localization, an interference effect with no classical analogue, because the trapping potential is always smaller than the kinetic energy.

One can thus expect at $E = E_{FB}$ different power laws compared to the conventional Anderson model, originating from the Cauchy-tailed effective disorder potential. Heavy tails also persist for small detunings $|E - E_{FB}| = \delta$ from E_{FB}, as long as $\delta \lesssim W$ and $E - E_{FB} - \epsilon_n^+ = 0$ has a solution. For small shifts, one can thus expect a crossover in scaling behaviour at $W \sim \delta$, *e.g.* from $\nu = 1$ to $\nu = 2$.

When E_{FB} is positioned in a gap, the dispersive states are evanescent even for vanishing disorder, and the distance from E_{FB} to the dispersive band edge sets the localization length similar to a defect state. Weak disorder merely determines the degree of hybridization between the evanescent waves and CLS. Hence we expect an exponent $\nu = 0$, with a nonzero finite $\xi(W \to 0)$ determined by the detuning of the flat band from the dispersive band edge.

Moving to higher dimensional lattices, $d > 1$, this Fano resonance picture will persist. It is, however, always possible for waves to travel around a resonant Fano state, so Anderson-localized dispersive waves cannot be trapped by Fano resonances and conventional scaling of ξ is expected. On the other hand, the enhancement of intensity at resonance can still influence other measures of localization, such as the eigenmode participation number $P = 1/\sum_n |\Psi_n|^4$, which counts the number of strongly excited lattice sites.

All results from above have to be compared to the impact of the coupling of CLS amongst each other ($U > 1$) or to the potential coupling between CLS and CLL. The network of weakly coupled and disordered CLS ($U > 1$) will yield a localization length which is independent of the disorder strength in the limit of weak disorder, since both the CLS-CLS coupling matrix elements and the CLS energy detuning are proportional to W. This effect will therefore be of potential importance only for flat bands located in gaps, and the corresponding localization length has to be compared to the above discussed one which originates from the coupling between gapped CLS and dispersive states. As for the coupling between CLS and CLL, we have to refer to future work, as this aspect is currently not understood in detail.

IV. EXAMPLES

We now apply the above formalism to some 1D examples generalizing the cross-stitch lattice studied in Ref. [26]. In particular, we consider the effect of onsite disorder on lattices with multiple flat bands (1D py-

rochlore) and flat bands of class $U = 2$ (stub and 1D Lieb), and the effect of coupling disorder in the tunable diamond ladder.

A. 1D Pyrochlore

As an example of a $U = 1$ flat band lattice, we consider the 1D pyrochlore lattice of Fig. 2(a). Its amplitude equations read

$$\begin{aligned} E\,a_n &= \epsilon_n^a a_n - b_n - b_{n-1} - d_n - c_{n-1},\\ E\,b_n &= \epsilon_n^b b_n - a_n - c_n - a_{n+1} - d_{n+1},\\ E\,c_n &= \epsilon_n^c c_n - b_n - d_n - a_{n+1} - d_{n+1},\\ E\,d_n &= \epsilon_n^d d_n - a_n - c_n - b_{n-1} - c_{n-1}. \end{aligned} \tag{3}$$

In the absence of the onsite potential ϵ, there are two flat bands and two dispersive bands,

$$E_{FB} = \{0, 2\}\,, \quad E(k) = -1 \mp \sqrt{5 + 4\cos k},$$

plotted in Fig. 2(b). The first CLS ($E_{FB,1} = 0$) is

$$a_n = b_n = \frac{1}{2}\delta_{n,m}, \quad c_n = d_n = -\frac{1}{2}\delta_{n,m}$$

with a corresponding four-dimensional local basis vector of $\vec{e}_{\mathrm{CLS},1} = (1, -1, 1, -1)/2$. The second CLS ($E_{FB,2} = 2$) is

$$a_n = c_n = \frac{1}{2}\delta_{n,m}, \quad b_n = d_n = -\frac{1}{2}\delta_{n,m}$$

with a local basis vector of $\vec{e}_{\mathrm{CLS},2} = (1, 1, -1, -1)/2$. These two local basis vectors define two Fano states $f_{\{1,2\},n}$ for each unit cell,

$$\begin{aligned} f_{\{1,2\},n} &= \frac{1}{2}(a_n \mp b_n \pm c_n - d_n),\\ \epsilon_n^{f_{\{1,2\}}} &= \frac{1}{4}(\epsilon_n^a \mp \epsilon_n^b \pm \epsilon_n^c - \epsilon_n^d) \end{aligned}$$

while the remaining two-dimensional orthogonal subspace spanned by $\vec{e}_\perp$ encodes the two remaining dispersive degrees of freedom $p_{\{1,2\},n}$, corresponding to the two dispersive spectral branches of Fig. 2(b),

$$\begin{aligned} p_{\{1,2\},n} &= \frac{1}{2}(a_n \pm b_n \pm c_n + d_n),\\ \epsilon_n^{p_{\{1,2\}}} &= \frac{1}{4}(\epsilon_n^a \pm \epsilon_n^b \pm \epsilon_n^c + \epsilon_n^d). \end{aligned}$$

These transformations can be encoded in the local rotation $\hat{D}$,

$$\hat{D} = \frac{1}{2}\begin{pmatrix} 1 & 1 & 1 & 1\\ 1 & -1 & -1 & 1\\ 1 & -1 & 1 & -1\\ 1 & 1 & -1 & -1 \end{pmatrix}, \tag{4}$$

with $(p_{1,n}, p_{2,n}, f_{1,n}, f_{2,n}) = \hat{D}(a_n, b_n, c_n, d_n)$, and the diagonal disorder terms transforming to $\hat{D}\mathrm{diag}(\epsilon_n^j)\hat{D}^{-1}$ (here $\mathrm{diag}(\epsilon_n^j)$ denotes a diagonal matrix with elements ϵ_n^j on the diagonal). The transformed disorder thus has both diagonal and off-diagonal components. Rewriting Eq. (3) in terms of the detangled variables, we obtain an equivalent set of amplitude equations,

$$\begin{aligned} Ef_{1,n} &= (\epsilon_n^{p_1} + 2)\, f_{1,n} + \epsilon_n^{p_2} f_{2,n} + \epsilon_n^{f_1} p_{1,n} + \epsilon_n^{f_2} p_{2,n},\\ Ef_{2,n} &= \epsilon_n^{p_2} f_{1,n} + \epsilon_n^{p_1} f_{2,n} + \epsilon_n^{f_2} p_{1,n} + \epsilon_n^{f_1} p_{2,n},\\ Ep_{1,n} &= \epsilon_n^{f_1} f_{1,n} + \epsilon_n^{f_2} f_{2,n} + (\epsilon_n^{p_1} - 2)\, p_{1,n} + \epsilon_n^{p_2} p_{2,n} -\\ &\quad p_{1,n-1} - p_{1,n+1} + p_{2,n-1} - p_{2,n+1},\\ Ep_{2,n} &= \epsilon_n^{f_2} f_{1,n} + \epsilon_n^{f_1} f_{2,n} + \epsilon_n^{p_2} p_{1,n} + \epsilon_n^{p_1} p_{2,n} +\\ &\quad p_{2,n-1} + p_{2,n+1} - p_{1,n-1} + p_{1,n+1}, \end{aligned} \tag{5}$$

corresponding to the "detangled" lattice in Fig. 2(c). Note in particular the structure of the effective coupling terms: symmetric parts yielding effective onsite potentials, and antisymmetric parts locally coupling the Fano states to the dispersive degrees of freedom, exactly as advertised in the previous section.

Hence if the potential satisfies the local symmetry $\epsilon_n^{f1} = \epsilon_n^{f2} = 0$ then the two CLS $f_{\{1,2\},n}$ decouple from the dispersive degrees of freedom $p_{\{1,2\},n}$. If that symmetry is additionally supported on all unit cells, then all CLS decouple with the individual energies

$$E = 1 + \epsilon_n^{p1} \pm \sqrt{1 + \left(\epsilon_n^{p2}\right)^2}.$$

Note that if $\epsilon_n^{p2} \neq 0$, the two CLS hybridize, but retain their compactness otherwise.

Because the coupling to the CLS is purely *local*, one can use the first two lines of Eq. (5) to eliminate the $f_{\{1,2\},n}$ variables for *arbitrary* ϵ_n, leaving equations for the dispersive variables $p_{\{1,2\},n}$ subject to a resonantly-enhanced effective disorder potential, in the same manner as the previous section. We hence expect quantities such as the localization length to be modified by an effective Cauchy-tailed disorder.

We verify this by numerically calculating the localization length $\xi(W)$ using the transfer number method outlined in the Appendix, assuming uncorrelated and uniformly distributed disorder $\epsilon \in [-W/2, W/2]$, where W is the disorder strength. We consider the scaling of ξ with W at different energies in Fig. 2(d). Away from the flat bands, we observe the usual $\nu = 2$ and $\nu = 2/3$ within and at band edges respectively, while at each of the flat band energies an anomalous $\nu = 1/2$ is observed. Thus, the Fano model remains applicable to lattices with multiple flat bands, where the disorder introduces (weak) hybridization between their CLS.

B. 1D Stub

For our second example we consider the 1D stub lattice shown in Fig. 3(a), which is of class $U = 2$. Its eigenmode

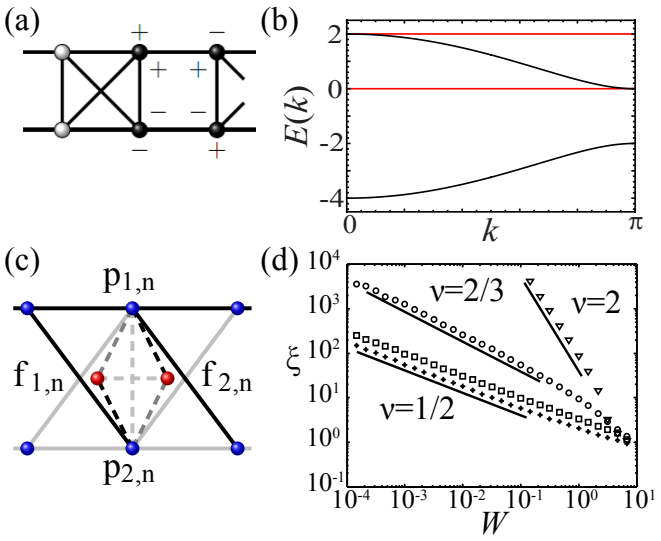

FIG. 2. (a) The 1D pyrochlore lattice. Circles denote lattice sites, solid lines are hopping (off-diagonal) elements with strength 1. Filled circles show profile of a compact localized state, with alternating signs its amplitudes as indicated. (b) Irreducible band structure, for onsite energies $\epsilon = 0$. (c) Equivalent lattice detangled by Eq. (5). Solid lines indicate dispersive coupling terms (grey lines carry the opposite sign as compared to the black ones), while the dashed disorder-induced coupling terms are, from lightest to darkest, $\{\epsilon_n^{p2}, \epsilon_n^{f1}, \epsilon_n^{f1}\}$. (d) Scaling of Anderson localization length ξ with disorder strength W, $\xi \sim 1/W^\nu$, for different energies E. Solid lines mark different power law exponents ν. $E = -2$ (circles, $\nu = 2/3$), $E = 0$ (squares, $\nu = 1/2$), $E = 2$ (*, $\nu = 1/2$), $E = 1$ (triangles, $\nu = 2$).

equations are

$$\begin{aligned} Ea_n &= \epsilon_n^a a_n - b_{n-1} - b_n - c_n, \\ Eb_n &= \epsilon_n^b b_n - a_n - a_{n+1}, \\ Ec_n &= \epsilon_n^c c_n - a_n, \end{aligned} \tag{6}$$

with spectrum (for $\epsilon = 0$)

$$E_{FB} = 0, \quad E(k) = \pm\sqrt{3 + 2\cos k},$$

plotted in Fig. 3(b). A CLS occupies a minumum of two unit cells,

$$a_n = 0,\ b_n = -\frac{1}{\sqrt{3}}\delta_{n,m},\ c_n = \frac{1}{\sqrt{3}}(\delta_{n,m} + \delta_{n,m+1}).$$

To detangle the lattice, we introduce a supercell formed by two unit cells, and perform rotations in the 3-dimensional subspace occupied by the CLS (leaving the a_n sublattice invariant). This detangling will only account for half of the flat band states, and we wish to determine whether this partial detangling is sufficient to understand the properties of the disordered system. The transformed amplitudes

$$\begin{aligned} f_n &= \frac{1}{\sqrt{3}}(c_{2n-1} - b_{2n-1} + c_{2n}), \\ p_{1,n} &= \frac{1}{\sqrt{2}}(c_{2n-1} - c_{2n}), \\ p_{2,n} &= \frac{1}{\sqrt{6}}(c_{2n-1} + 2b_{2n-1} + c_{2n}), \end{aligned}$$

correspond to the local rotation $(p_{1,n}, p_{2,n}, f_n) = \hat{D}(c_{2n-1}, b_{2n-1}, c_{2n})$ with

$$\hat{D} = \begin{pmatrix} \frac{1}{\sqrt{2}} & 0 & -\frac{1}{\sqrt{2}} \\ \frac{1}{\sqrt{6}} & \frac{2}{\sqrt{6}} & \frac{1}{\sqrt{6}} \\ \frac{1}{\sqrt{3}} & -\frac{1}{\sqrt{3}} & \frac{1}{\sqrt{3}} \end{pmatrix}. \tag{7}$$

Similarly transforming the potentials,

$$\begin{aligned} \epsilon_n^f &= \frac{1}{3}(\epsilon_{2n-1}^c + \epsilon_{2n-1}^b + \epsilon_{2n}^c), \\ \epsilon_n &= \frac{1}{\sqrt{6}}(\epsilon_{2n-1}^c - \epsilon_{2n}^c), \\ \gamma_n &= \frac{1}{3\sqrt{2}}(\epsilon_{2n-1}^c - 2\epsilon_{2n-1}^b + \epsilon_{2n}^c), \end{aligned}$$

and substituting into Eq. (6), we obtain the equivalent detangled lattice

$$\begin{aligned} Ef_n &= \epsilon_n^f f_n + \epsilon_n\, p_{1,n} + \gamma_n\, p_{2,n}, \\ Ep_{1,n} &= \epsilon_n f_n + \left(\epsilon_n^f + \frac{\gamma_n}{\sqrt{2}}\right) p_{1,n} + \frac{\epsilon_n}{\sqrt{2}}\, p_{2,n} \\ &\quad + \frac{1}{\sqrt{2}}\,(a_{2n} - a_{2n-1})\,, \\ Ep_{2,n} &= \gamma_n f_n + \frac{\epsilon_n}{\sqrt{2}}\, p_{1,n} + \left(\epsilon_n^f - \frac{\gamma_n}{\sqrt{2}}\right) p_{2,n} \\ &\quad - \sqrt{\frac{3}{2}}\,(a_{2n-1} + a_{2n})\,, \\ Ea_{2n-1} &= \epsilon_{2n-1}^a a_{2n-1} - b_{2n-2} - \frac{1}{\sqrt{2}} p_{1,n} - \sqrt{\frac{3}{2}} p_{2,n}, \\ Ea_{2n} &= \epsilon_{2n}^a a_{2n} - b_{2n} + \frac{1}{\sqrt{2}} p_{1,n} - \sqrt{\frac{3}{2}} p_{2,n}, \\ Eb_{2n} &= \epsilon_{2n}^b b_{2n} - a_{2n} - a_{2n+1}, \end{aligned} \tag{8}$$

illustrated in Fig. 3(c). The $p_{1,j}, p_{2,j}$ sites form two separate paths between the a_{2j-1} and a_{2j} sites; destructive interference between these paths can suppress wave transport, corresponding to the "missing" flat band states not included in our detangling. In fact, these missing states form a flat band of class $U = 2$ in the detangled lattice; thus by repeatedly applying the detangling procedure one can isolate a larger fraction of the FBS to identify symmetries in the disorder potential that leave them decoupled. For example, the detangled Fano states f_j are completely decoupled from the chain in the absence of disorder, and they remain decoupled if the disorder has the local symmetry $\epsilon_n = \gamma_n = 0$.

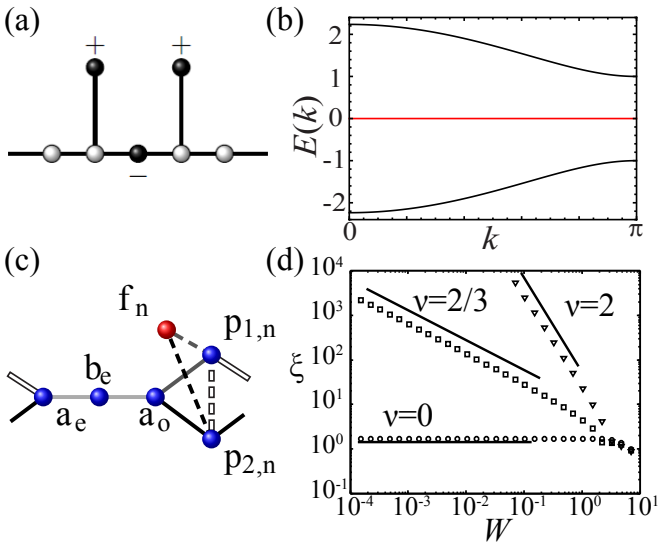

FIG. 3. (a) The stub lattice. Circles denote lattice sites, solid lines are hopping (off-diagonal) elements with strength 1. Filled circles show profile of a compact localized state, with alternating signs its amplitudes as indicated. (b) Irreducible band structure, for onsite energies $\epsilon = 0$. (c) Equivalent lattice detangled by Eq. (8). Dispersive couplings are $\pm\sqrt{1/2}, -1, -\sqrt{3/2}$ (from light to dark). The disorder-induced couplings are respectively $\epsilon_n/\sqrt{2}, \epsilon_n, \gamma_n$ (from light to dark). To conserve space, the notations $a_e = a_{2n-2}, b_e = b_{2n-2}, a_o = a_{2n-1}$ have been used. (d) Scaling of Anderson localization length ξ with disorder strength W, $\xi \sim 1/W^\nu$, for different energies E. Solid lines mark different power law exponents ν. $E = 0$ (circles, $\nu = 0$), $E = 1$ (squares, $\nu = 2/3$), $\sqrt{2}$ (triangles, $\nu = 2$).

Turning to the scaling of the localization length in Fig. 2(d), since the flat band is isolated from the dispersive band by a gap, there is no scaling at E_{FB} ($\nu = 0$), and the dispersive band displays the expected exponents $\nu = 2/3$ and 2. Moving slightly away from E_{FB}, nontrivial behaviour of $\xi(E, W)$ induced by a gapped flat band was recently reported in Ref. [20]: the decay of ξ as $|E - E_{FB}|$ increases is nonmonotonic.

C. 1D Lieb

As a second example of class $U = 2$ we consider the 1D Lieb lattice shown in Fig. 4(a). Its eigenmode equations

$$\begin{aligned} Ea_n &= \epsilon_n^a a_n - d_{n-1} - d_n - e_n, \\ Eb_n &= \epsilon_n^b b_n - c_{n-1} - c_n - e_n, \\ Ec_n &= \epsilon_n^c c_n - b_n - b_{n+1}, \\ Ed_n &= \epsilon_n^d d_n - a_n - a_{n+1}, \\ Ee_n &= \epsilon_n^e e_n - a_n - b_n, \end{aligned} \tag{9}$$

yield (for $\epsilon = 0$) the spectrum

$$E_{FB} = 0,\ E(k) = \left\{ \pm\sqrt{2 + 2\cos k}, \pm\sqrt{4 + 2\cos k} \right\},$$

plotted in Fig. 4(b). In contrast to the stub lattice, the Lieb lattice has dispersive bands in resonance with its flat band, so we anticipate nontrivial scaling of its localization length. The flat band's CLS is

$$a_n = b_n = 0,\ c_n = d_n = \frac{1}{2}\delta_{n,m},\ e_n = \frac{1}{2}(\delta_{n,m} + \delta_{n,m+1}).$$

Applying the transformation

$$\{\bar{a}_n, \bar{c}_n\} = \frac{1}{\sqrt{2}}(a_n \mp b_n), \quad \{\bar{b}_n, \bar{d}_n\} = \frac{1}{\sqrt{2}}(d_n \mp c_n)$$

corresponding to the rotation

$$\hat{D} = \frac{1}{\sqrt{2}} \begin{pmatrix} 1 & -1 & 0 & 0 & 0 \\ 0 & 0 & -1 & 1 & 0 \\ 1 & 1 & 0 & 0 & 0 \\ 0 & 0 & 1 & 1 & 0 \\ 0 & 0 & 0 & 0 & \sqrt{2} \end{pmatrix},$$

and similarly transforming the disorder potential by $\hat{D}\mathrm{diag}(\epsilon_n^j)\hat{D}^{-1}$,

$$\epsilon_n^{1\pm} = \frac{1}{2}(\epsilon_n^a \pm \epsilon_n^b), \quad \epsilon_n^{2\pm} = \frac{1}{2}(\pm\epsilon_n^c + \epsilon_n^d),$$

we obtain the partially-detangled lattice

$$\begin{aligned} E\bar{a}_n &= \epsilon_n^{1+}\bar{a}_n - \bar{b}_{n-1} - \bar{b}_n + \epsilon_n^{1-}\bar{c}_n, \\ E\bar{b}_n &= \epsilon_n^{2+}\bar{b}_n - \bar{a}_n - \bar{a}_{n+1} + \epsilon_n^{2-}\bar{d}_n, \\ E\bar{c}_n &= \epsilon_n^{1+}\bar{c}_n + \epsilon_n^{1-}\bar{a}_n - \bar{d}_{n-1} - \bar{d}_n - e_n\sqrt{2}, \\ E\bar{d}_n &= \epsilon_n^{2+}\bar{d}_n + \epsilon_n^{2-}\bar{b}_n - \bar{c}_n - \bar{c}_{n+1}, \\ Ee_n &= \epsilon_n^e e_n - \bar{c}_n\sqrt{2}, \end{aligned} \tag{10}$$

shown in Fig. 4(c). It consists of an ordinary 1D chain with $(\bar{a}_n, \bar{b}_n)$ sites, corresponding to the middle two dispersive bands, coupled via disorder to a 1D stub lattice. One could further detangle this stub lattice is a manner similar to the calculations above, but this partial detangling is already sufficient to understand the effect of disorder.

In contrast to the previous examples, in the Lieb lattice there are two possible transmission channels for the dispersive waves, corresponding to either $(\bar{a}_n, \bar{b}_n)$ or $(\bar{c}_n, \bar{d}_n)$ chains, leading to two distinct localization lengths which can be computed using the transfer matrix method outlined in the Appendix. The observed power law scalings in Fig. 4(d) show some interesting features caused by either the resonant interaction between CLS and a dispersive channel, or between the two dispersive channels.

At E_{FB} there are two exponents: $\nu = 0$, and $\nu \approx 4/3$. The $\nu = 0$ exponent corresponds to transmission along the "stub" part of the detangled lattice; since its flat band is separated by a gap, there is no scaling of its localization length, as expected. On the other hand, modes of the $(\bar{a}_n, \bar{b}_n)$ chain are in resonance with the stub's flat band states, leading to a Fano resonance-induced modification to its scaling. Since the CLS do not excite the $\bar{c}_n$ sublattice, disorder can only directly couple the Fano states to

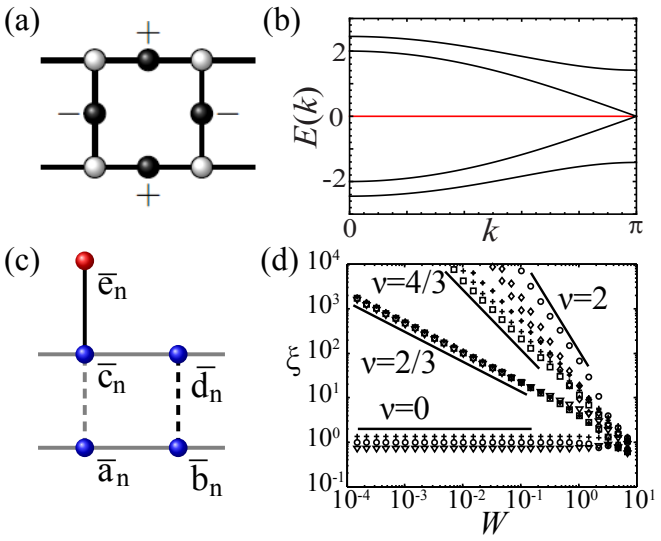

FIG. 4. (a) The 1D Lieb lattice. Circles denote lattice sites, solid lines are hopping (off-diagonal) elements with strength 1. Filled circles show profile of a compact localized state, with alternating signs its amplitudes as indicated. (b) Irreducible band structure, for onsite energies $\epsilon = 0$. (c) Equivalent lattice detangled by Eq. (10). The fixed couplings are $-1, -\sqrt{2}$ (light/dark). The disorder-induced couplings are ϵ_n^{1-} (light) and ϵ_n^{2-} (dark) (d) Scaling of Anderson localization length ξ with disorder strength W, $\xi \sim 1/W^\nu$, for different energies E. Solid lines mark different power law exponents ν. $E = 0$ (+, $\nu = 0, 4/3$), $E = 1$ (circles, $\nu = 0, 2$), $\sqrt{2}$ (*, $\nu = 2/3, 4/3$), $E = 1.8$ (diamonds, $\nu = 2, 2$), $E = 2$ (squares, $\nu = 2/3, 4/3$), $E = \sqrt{6}$ (triangles, $\nu = 0, 2/3$).

the $\bar{b}_n$ sublattice, *i.e.* there is only a Fano resonance at every *second* lattice site. This resembles the geometry of the diamond ladder studied extensively in Ref. [19], and remarkably we obtain the same scaling exponent $\nu \approx 4/3$ even though the physical lattice is completely different.

A second pair of anomalies occur at the energies $E = \sqrt{2}, 2$, which both have exponents $\nu = 2/3, 4/3$. At these energies one of the dispersive channels has a band edge, corresponding to exponent $\nu = 2/3$. Interestingly, the vanishing group velocity and stronger localization associated with these band edge states presumably leads to the resonantly-enhanced $\nu = 4/3$ exponent for the mid-band states in the other dispersive channel (a full analysis of the resonant interaction between multiple dispersive channels is however beyond the scope of this work). All other energies display conventional exponents.

D. 1D Tunable Diamond: Off-diagonal disorder

As a final application of the Fano detangling procedure in 1D, we consider off-diagonal disorder [36]. In ordinary lattices, off-diagonal disorder has a significantly different effect compared to diagonal disorder: modes at the band centre $E = 0$ become delocalized [37–39]. However in our case, the Fano rotations generically mix disorder terms into a combination of effective onsite and hopping disorder. Thus, pure hopping disorder and pure onsite disorder have qualitatively similar effects, so there are no delocalized states at E_{FB}. As an explicit example, consider the $U = 1$ diamond ladder with hopping disorder shown in Fig. 5(a). Its eigenmode equations read

$$\begin{aligned} Ea_n &= -C_{1,n}b_n - C_{3,n}b_{n+1} - C_{5,n}c_n, \\ Eb_n &= -C_{3,n-1}a_{n-1} - C_{1,n}a_n - C_{4,n-1}c_{n-1} - C_{2,n}c_n, \\ Ec_n &= -C_{2,n}b_n - C_{4,n}b_{n+1} - C_{5,n}a_n, \end{aligned} \tag{11}$$

where the hopping is taken from uniformly distributed random variables $C_{1-4,n} \in 1 + [-W/2, W/2]$, and $C_{5,n} \in t + [-W/2, W/2]$. To ensure positive nonzero couplings – generally the case for ordinary evanescently coupled waveguide arrays – we enforce the restriction $W < \lfloor t, 1 \rfloor$. In the ordered case $W = 0$ the cross coupling term $C_{5,n}$ shifts the energy of the flat band to $E_{FB} = t$, opening a gap between the two dispersive bands, see eg. Fig. 5(b) showing the spectrum for $t = 1$. When $t > 2$, E_{FB} becomes separated from dispersive bands by a gap.

We reduce the eigenvalue problem to the Fano form by making the rotation

$$f_n = \frac{C_{4,n}a_n - C_{3,n}c_n}{\sqrt{C_{3,n}^2 + C_{4,n}^2}}, \quad p_n = \frac{C_{3,n}a_n + C_{4,n}c_n}{\sqrt{C_{3,n}^2 + C_{4,n}^2}},$$

corresponding to $(p_n, f_n) = \hat{D}(a_n, c_n)$ with

$$\hat{D} = \frac{1}{\sqrt{C_{3,n}^2 + C_{4,n}^2}} \begin{pmatrix} C_{4,n} & -C_{3,n} \\ C_{3,n} & C_{4,n} \end{pmatrix}. \tag{12}$$

Notably, here the detangling itself depends on the disorder. The eigenmode equations become

$$\begin{aligned} (E - C_{5,n})f_n &= -\tilde{C}_{2,n}b_n - \tilde{C}_{4,n}p_n, \\ (E + C_{5,n})p_n &= -\tilde{C}_{3,n}b_n - \tilde{C}_{1,n}b_{n+1} - \tilde{C}_{4,n}f_n, \\ Eb_n &= -\tilde{C}_{2,n}f_n - \tilde{C}_{3,n}p_n - \tilde{C}_{1,n-1}p_{n-1}, \end{aligned} \tag{13}$$

where we have introduced the effective couplings

$$\begin{aligned} \tilde{C}_{1,n} &= \sqrt{C_{3,n}^2 + C_{4,n}^2}, \\ \tilde{C}_{2,n} &= (C_{1,n}C_{4,n} - C_{2,n}C_{3,n})/\tilde{C}_{1,n}, \\ \tilde{C}_{3,n} &= (C_{1,n}C_{3,n} + C_{2,n}C_{4,n})/\tilde{C}_{1,n}, \\ \tilde{C}_{4,n} &= C_{5,n}(C_{4,n}^2 - C_{3,n}^2)/(2C_{3,n}C_{4,n}). \end{aligned} \tag{14}$$

This Fano form is illustrated in Fig.5(c). The off-diagonal disorder is transformed to a mixture of effective on-site and hopping disorder. The Fano states have energy $C_{5,n}$ and are coupled to *both* sublattices of the dispersive chain. In the limit of vanishing disorder, $\tilde{C}_{2,n}, \tilde{C}_{4,n} \to 0$. Then $\tilde{C}_{1,n}, \tilde{C}_{3,n} \to \sqrt{2}$ and coupling to the Fano state vanishes. Such Fano decoupling also occurs if the disorder is correlated such that $C_{1,n} = C_{2,n}$ and $C_{3,n} = C_{4,n}$.

Eliminating the Fano sites f_n, we obtain

$$Ep_n = \epsilon_{1,n}p_n - \tilde{C}_{0,n}b_n - \tilde{C}_{1,n}b_{n+1},$$
$$Eb_n = \epsilon_{2,n}b_n - \tilde{C}_{0,n}p_n - \tilde{C}_{1,n-1}p_{n-1},$$

where

$$\epsilon_{1,n} \equiv \frac{\tilde{C}_{4,n}^2}{E + C_{5,n}} + C_{5,n}, \quad \epsilon_{2,n} \equiv \frac{\tilde{C}_{2,n}^2}{E + C_{5,n}},$$
$$\tilde{C}_{0,n} \equiv \tilde{C}_{3,n} + \frac{\tilde{C}_{2,n}\tilde{C}_{4,n}}{E + C_{5,n}},$$

which is similar to the onsite disorder case, as expected. In particular, for weak disorder we have $\tilde{C}_{2,n}, \tilde{C}_{4,n} \sim W$ and the Fano resonance leads to a divergence of the effective onsite potentials $\varepsilon_{j,n}$ when $E = C_{5,n}$. In the disordered system this can occur within the resonance width $|E - E_{FB}| < W/2$, leading again to an effective disorder potential with Cauchy tails and a much smaller localization length. Outside this window, the effective onsite disorder is bounded with (nonzero) strength proportional to W. Consequently, there should be no divergence of ξ for the dispersive states, which is completely different from the conventional Anderson model with hopping disorder.

As above, we test these predictions by numerically calculating $\xi(E, W)$ using the transfer number method. We find indeed that $\xi(E)$ shows no divergences, and calculate the weak disorder power law scalings at E_{FB} for different flat band positions (choices of t) in Fig. 5. In all cases, the predicted anomalous scaling laws at E_{FB} are observed ($\nu = 1, 1/2$ or 0), in contrast to the $\nu = 2$ off-resonance with the flat band. Thus, as anticipated, hopping disorder has an effect qualitatively similar to onsite disorder.

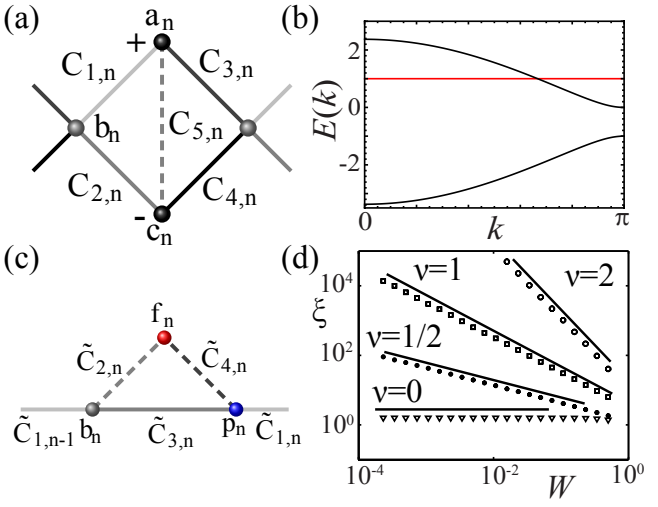

FIG. 5. (a) The 1D diamond ladder. Circles denote lattice sites, solid lines are hopping (off-diagonal) elements with random strength. Filled circles show profile of a compact localized state, with alternating signs its amplitudes as indicated. (b) Irreducible band structure, for $t = 1$ and onsite energies $\epsilon = 0$. (c) Equivalent lattice detangled by Eq. (13). (d) Scaling of Anderson localization length ξ with disorder strength W, $\xi \sim 1/W^\nu$, for different energies E. Solid lines mark different power law exponents ν. $E = 1.5, t = 1$ (circles, $\nu = 2$), $E = t = 1$ (squares, $\nu = 4/3$), $E = t = 2$ (*, $\nu = 1/2$), $E = t = 2.1$ (triangles, $\nu = 0$).

V. 2D LATTICES

We now examine how the detangling concept generalizes to 2D lattices. Fig. 6 shows examples of 2D flat band lattices along with their CLS and irreducible band structures. For $U = 1$ lattices such as the cross-stitch, the position of the flat band with respect to dispersive bands is tunable, whereas in the $U > 1$ examples (2D Lieb, 2D pyrochlore, and Kagome) the flat band is forced to touch the edge of a dispersive band. These "protected" crossings are a consequence of the real space topology of the CLS, which form a linearly dependent set. The "missing" flat band states resulting from this linear dependence belong to the touching dispersive band, which cannot be gapped out without destroying the CLS [25].

As noted above, in dimensions $d > 1$ it is always possible for a dispersive wave to travel around a strong yet localized Fano scatterer, which spoils the trapping mechanism responsible for the anomalous scaling of the localization length in 1D. We thus expect on one hand conventional scaling of the localization length ξ in these 2D examples, *i.e.* marginal localization with an essential singularity as $W \to 0$ [31].

On the other hand, resonances still result in very strongly excited sites, which influences other measures of eigenmode localization such as the participation number $P = 1/\sum_n |\Psi_n|^4$. P counts the number of sites strongly excited in an eigenmode Ψ_n, and in conventional lattices it is proportional to the localization volume $(\xi)^d$. In a weakly disordered flat band, P should instead count the number of Fano resonances, $\sim W(\xi)^d$, which is much smaller than the localization volume in the weak disorder limit [26].

To test this prediction, we carry out exact diagonlization of the disordered $t = 4$ cross-stitch and pyrochlore lattices. In both cases the flat band touches the edge of the dispersive band. For eigenmodes near the flat band energy E_{FB}, we compute three measures: P, $P_{\rm FB}$, and $P_{\rm disp}$. $P_{\rm FB}$ is the participation number of the normalized flat band component of the eigenmode, which estimates the number of resonances. Similarly the participation number of the eigenmodes projected onto the dispersive bands $P_{\rm disp}$ estimates the localization volume, $P_{\rm disp} \sim (\xi)^d$. Fig. 7 shows the scaling of these three measures with disorder strength W.

For the cross-stitch case we indeed see that P counts the number of resonances $\sim P_{FB}$ rather than the localization volume $\sim P_{\rm disp}$, which grows much more rapidly as $W \to 0$. The slower growth of $P_{\rm FB}$ is consistent with the number of resonances growing as $P_{\rm Fano} \propto W(\xi)^d$. On

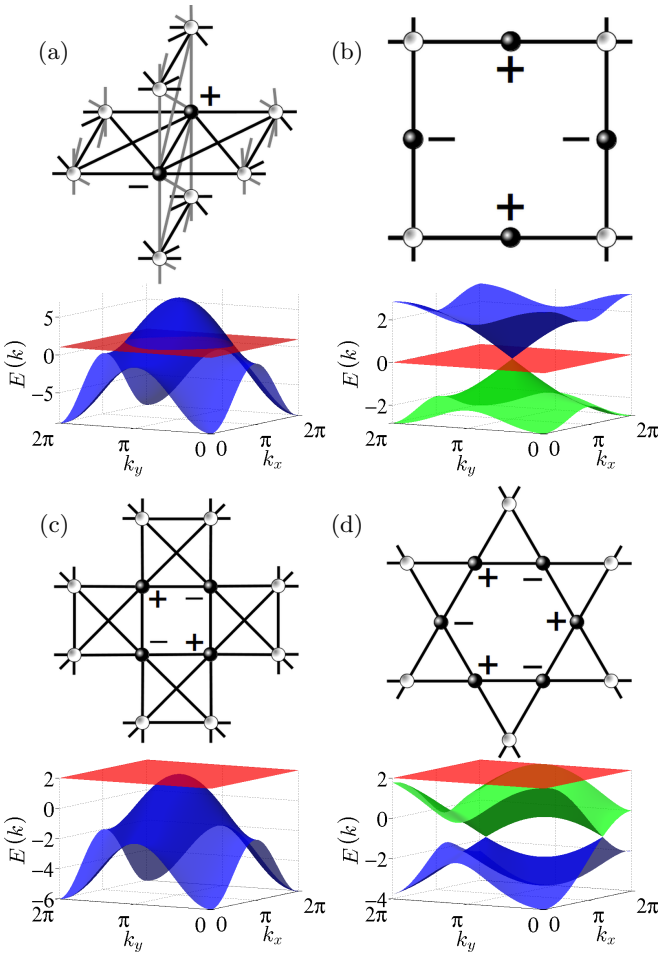

FIG. 6. Two-dimensional FB lattices. Circles denote lattice sites, black/grey lines are hopping (off-diagonal) elements of $t = 1$. Filled circles again show CLS location. Irreducible band structures for onsite energies $\epsilon = 0$ are shown below each lattice, with flat bands corresponding to red horizontal planes. The models and CLS classes are: (a) 2-D cross-stitch, $U = 1$ (black/grey lines denote horizontal/vertical bonding); (b) Lieb, $U = 3$; (c) pyrochlore, $U = 3$; and (d) Kagome, $U = 4$.

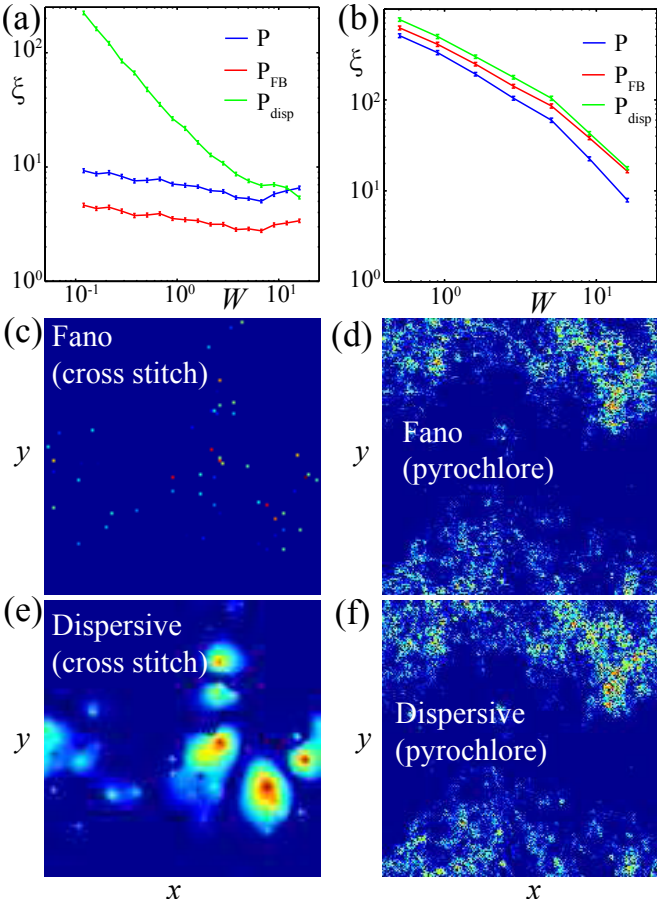

FIG. 7. Flat band Anderson localization in the 2D cross-stitch (a,c,e) and pyrochlore (b,d,f) lattices. (a,b) Scaling of eigenmode participation number P with disorder strength W at E_{FB}, along with its flat band $P_{\rm FB}$ and dispersive components $P_{\rm disp}$. The lattice width is 300 unit cells and error bars indicate statistical error. (c–f) Representative intensity profiles of FB (c,d) and dispersive (e,f) components of a weak disorder ($W = 0.1$) eigenmode.

the other hand, in the 2D pyrochlore we see a distinctly different behaviour, with $P \sim P_{\rm Fano} \sim P_{\rm disp}$ all growing at similar rates as $W \to 0$. Thus, the predicted scaling of the number of resonances in an eigenmode breaks down at a protected crossing.

To further demonstrate this strong qualitative difference, we consider the profiles of the flat band and dispersive band components of a representative eigenmode at E_{FB} in Fig. 7(c-f). We observe very different mode profiles; the cross-stitch eigenmodes agree with our intuition, consisting of a collection of well-separated resonant CLS, weakly coupled via the Anderson-localized dispersive states. In contrast, this weak coupling assumption is violated in the 2D pyrochlore; many CLS are excited in close proximity and they can no longer be considered independently. Similar behaviour also occurs in 2D Lieb and Kagome lattices which also host protected band crossings.

This strong coupling between Fano scatterers is mediated by the delocalized dispersive states that replace the "missing" CLS at a protected band crossing. The coupling can be quantified by considering the range of the (real space) flat band projection operator, which determines how the CLS respond to a local perturbation. In regular flat bands the projection operator is either local ($U = 1$) or short-ranged ($U > 1$); the disorder perturbs each CLS independently. However in $d > 1$ lattices with protected crossings, the projector is long-ranged with a power law decay $\sim 1/r^d$, leading to strong coupling, geometric frustration, and multifractality in the $W \to 0$ limit [18]; the CLS respond to generic perturbations in a complex way. We stress however that under suitable correlated perturbations that for example do not shift the energy of some fraction of the CLS, weakly coupled CLS

can persist [40].

VI. CONCLUSIONS

We have shown that the "compact localized state" picture of flat band eigenmodes provides a useful way to understand the response of a variety of flat band lattices to perturbations such as disorder, testing the prediction of a Fano resonance-enhanced effective disorder potential against numerical computation of the Anderson localization length in four one-dimensional lattices with different properties. We have verified the applicability of this model to: (i) lattices with multiple flat bands, (ii) flat bands of class $U > 1$, where the minimal compact localized states occupy multiple unit cells, and (iii) lattices with off-diagonal (hopping) disorder.

In most cases, our reduction to the Lloyd model correctly predicts the scaling exponent ν of the localization length in 1D. While this reduction inexplicably fails for the 1D Lieb lattice flat band, for which $\nu \approx 4/3$, we found a reduction of this model to a previously studied case sharing the same anomalous exponent: the diamond ladder [19]. The appearance of $\nu = 4/3$ in dispersive bands in the Lieb lattice suggests a universal mechanism, probably related to the density of states, which would be interesting to explore further in future studies, either by applying the semi-analytical approach recently introduced in Ref. [20], or generalizing the older perturbative expansions of Refs. [35, 41, 42] to disorder with a divergent variance. We leave a rigorous analytical derivation of this anomalous scaling law as an open problem.

Generalizing to 2D lattices, we found that the response to disorder becomes sensitive the "geometric frustration" of the flat band. In certain "unfrustrated" lattices disorder weakly couples compact localized states via dispersive states, similar to the 1D case. On the other hand, in "frustrated" lattices the coupling between CLS becomes long-ranged and this simple picture of independent Fano resonances breaks down under generic uncorrelated disorder.

Finally, while we have focused on the case of static disorder potentials, our detangling procedure may also be useful in characterizing the response of flat bands to other perturbations, such as nonlinearities [43–45] or balanced gain and loss [45, 46].

ACKNOWLEDGEMENTS

This research was supported by the Australian Research Council, and the Singapore National Research Foundation under grant No. NRFF2012-02.

Appendix A: Localization length

In 1D lattices with only a single transmission channel (such as the sawtooth, pyrochlore, and stub), we can apply the simple transfer number method to obtain the localization length. This relies on the fact that a single scalar equation describes the growth rate of the eigenmodes. As an example, we consider the two-band approximation of Eq. (2). Dividing by the dispersive wave amplitude p_n, defining the amplitude ratio $R_n \equiv p_{n+1}/p_n$ and rearranging, we obtain the map

$$R_n = V_n + \frac{(\epsilon_n^-)^2}{E - E_{FB} - \epsilon_n^+} - E - \frac{1}{R_{n-1}}. \tag{A1}$$

For Anderson localized modes, $p_n \sim e^{n/\xi}$, where ξ is the localization length, such that $R_n \sim e^{1/\xi}$ and the localization length is obtained as [31]

$$\xi^{-1} = \lim_{N\to\infty} \frac{1}{N} \sum_{n=1}^{N} \ln |R_n|. \tag{A2}$$

For sufficiently large N the summand is self-averaging and this expression converges to ξ^{-1}.

In lattices with multiple ($M > 1$) transmission channels (eg. 1D Lieb and 2D lattices), each channel j has a different localization length ξ_j. If one eliminates variables to obtain a single equation for an amplitude ratio R_n, the solution will only be sensitive to the fastest growing channel, corresponding to the smallest localization length $\min(\xi_j)$, whereas the transport properties of the lattice are determined by the *largest* localization length. Thus, the transfer number method no longer works, and the more general transfer matrix method is required [31, 47]. Typically one writes the eigenvalue problem as

$$\hat{t}_n \psi_{n+1} = (\hat{\epsilon}_n - E)\psi_n - \hat{t}_{n-1}^\dagger \psi_{n-1}, \tag{A3}$$

where ψ_n encodes the sublattice amplitudes, $\hat{t}$ describes intercell hopping, and $\hat{\epsilon}$ accounts for intracell hopping and onsite potentials. This can be rewritten as

$$\begin{aligned} \begin{pmatrix} \psi_{n+1} \\ \psi_n \end{pmatrix} &= \begin{pmatrix} t_n^{-1}(\hat{\epsilon}_n - E) & -t_n^{-1} t_{n-1}^\dagger \\ \hat{1} & 0 \end{pmatrix} \begin{pmatrix} \psi_n \\ \psi_{n-1} \end{pmatrix}, \\ &= \hat{T} \begin{pmatrix} \psi_n \\ \psi_{n-1} \end{pmatrix}, \end{aligned} \tag{A4}$$

where $\hat{T}$ is the transfer matrix and $\hat{1}$ is the identity matrix. For sufficiently large N the localization lengths ξ_j are obtained from the M largest eigenvalues λ_j of $\hat{T}^N$ as $1/\xi_j = \frac{1}{N} \ln |\lambda_j|$. Note that a naive direct computation of the matrix T^N via matrix multiplication will suffer from numerical overflow, hence one must periodically orthonormalize columns of the partial product $\hat{T}^n$ [31].

[1] T. Brandes, *Coherent and collective quantum optical effects in mesoscopic systems*, Phys. Rep. **408**, 315 (2005).

[2] I. Bloch, J. Dalibard, and W. Zwerger, *Many-body physics with ultracold gases*, Rev. Mod. Phys. **80**, 885 (2008).

[3] M. Bellec, U. Kuhl, G. Montambaux, and F. Mortessagne, *Tight-binding couplings in microwave artificial graphene*, Phys. Rev. B **88**, 115437 (2013).

[4] D. N. Christodoulides, F. Lederer, and Y. Silberberg, *Discretizing light behavior in linear and nonlinear waveguide lattices*, Nature **424**, 817 (2003).

[5] E. J. Bergholtz and Z. Lu, *Topological flat band models and fractional Chern insulators*, Int. J. Mod. Phys. B **27**, 1330017 (2013).

[6] A. Parameswaran, R. Roy, and S. L. Sondhi, *Fractional quantum Hall physics in topological flat bands*, Comptes Rendus Physique **14**, 816 (2013).

[7] O. Derzhko and J. Richter, *Universal low-temperature behavior of frustrated quantum antiferromagnets in the vicinity of the saturation field*, Eur. Phys. J. **B 52**, 23 (2006); O. Derzhko, J. Richter, A. Honecker, M. Maksymenko, and R. Moessner, *Low-temperature properties of the Hubbard model on highly frustrated one-dimensional lattices*, Phys. Rev. **B 81**, 014421 (2010).

[8] M. Hyrkäs, V. Apaja and M. Manninen, *Many-particle dynamics of bosons and fermions in quasi-one-dimensional flat-band lattices*, Phys. Rev. **A 87**, 023614 (2013).

[9] O. Derzhko, J. Richter, and M. Maksymenko, *Strongly correlated flat-band systems: The route from Heisenberg spins to Hubbard electrons*, Int. J. Mod. Phys. B **29**, 1530007 (2015).

[10] D. Guzmán-Silva, C. Meijá-Cortés, M. A. Bandres, M. C. Rechtsman, S. Weimann, S. Nolte, M. Segev, A. Szameit, and R. A. Vicencio, *Experimental observation of bulk and edge transport in photonic Lieb lattices*, New. J. Phys. **16**, 063061 (2014).

[11] R. A. Vicencio, C. Cantillano, L. Morales-Inostroza, B. Real, C. Meijia-Cortes, S. Weimann, A. Szameit and M. I. Molina, *Observation of localized states in Lieb photonic lattices*, Phys. Rev. Lett. **114**, 245503 (2015).

[12] S. Mukherjee, A. Spracklen, D. Choudhury, N. Goldman, P. Öhberg, E. Andersson, and R. R. Thomson, *Observation of a localized flat-band state in a photonic Lieb lattice*, Phys. Rev. Lett. **114**, 245504 (2015).

[13] N. Masumoto, N. Y. Kim, T. Burnes, K. Kusudo, A. Löffler, S. Höfling, A. Forchel, and Y. Yamamoto, *Excitonpolariton condensates with flat bands in a two-dimensional kagome lattice*, New. J. Phys. **14**, 065002 (2012).

[14] F. Baboux, L. Ge, T. Jacqmin, M. Biondi, A. Lemaitre, L. Le Gratiet, I. Sagnes, S. Schmidt, H. E. Türeci, A. Amo, and J. Bloch, *Bosonic condensation and disorder-induced localization in a flat band*, arXiv:1505.05652 (2015).

[15] S. Taie, H. Ozawa, T. Ichinose, T. Nishio, S. Nakajima, and Y. Takahashi, *Coherent driving and freezing of bosonic matter in an optical Lieb lattice*, Science Advances **1**, e1500854 (2015).

[16] M. Goda, S. Nishino, and H. Matsuda, *Inverse Anderson transition caused by flatbands*, Phys. Rev. Lett. **96**, 126401 (2006).

[17] S. Nishino, H. Matsuda, and M. Goda, *Flat-band localization in weakly disordered system*, J. Phys. Soc. Jpn. **76**, 024709 (2007).

[18] J. T. Chalker, T. S. Pickles, and P. Shukla, *Anderson localization in tight-binding models with flat bands*, Phys. Rev. B **82**, 104209 (2010).

[19] D. Leykam, S. Flach, O. Bahat-Treidel, and A. S. Desyatnikov, *Flat band states: disorder and nonlinearity*, Phys. Rev. B, **88**, 224203 (2013).

[20] L. Ge and H. E. Tureci, *Energy dependence and scaling property of localization length near a gapped flat band*, arXiv:1509.00881.

[21] A. Mielke, J. Phys. A **24**, L73 (1991); **24**, 3311 (1991); **25**, 4335 (1992).

[22] H. Tasaki, *Ferromagnetism in the Hubbard models with degenerate single-electron ground states*, Phys. Rev. Lett. **69**, 1608 (1992).

[23] R. G. Dias and J. D. Gouveia, *Origami rules for the construction of localized eigenstates of the Hubbard model in decorated lattices*, Scientific Rep. **5**, 16852 (2015).

[24] A. Nandy and A. Chakrabarti, *Engineering flat electronic bands in quasiperiodic and fractal loop geometries*, Phys. Lett. A **379**, 2876 (2015).

[25] D. L. Bergman, C. Wu, and L. Balents, *Band touching from real-space topology in frustrated hopping models*, Phys. Rev. B **78**, 125104 (2008).

[26] S. Flach, D. Leykam, J. D. Bodyfelt, P. Matthies and A. S. Desyatnikov, *Detangling flat bands into Fano lattices*, EPL **105**, 30001 (2014).

[27] A. E. Miroshnichenko, S. Flach, and Yu. S. Kivshar, *Fano resonances in nanoscale structures*, Rev. Mod. Phys. **82**, 2257 (2010).

[28] L. I. Deych, A. A. Lisyansky, and B. L. Altshuler, *Single Parameter Scaling in One-Dimensional Localization Revisited*, Phys. Rev. Lett. **84**, 2678 (2000); *Single-parameter scaling in one-dimensional Anderson localization: Exact analytical solution*, Phys. Rev. B **64**, 224202 (2001).

[29] L. I. Deych, M. V. Erementchouk, A. A. Lisyansky, and B. L. Altshuler, *Scaling and the Center-of-Band Anomaly in a One-Dimensional Anderson Model with Diagonal Disorder*, Phys. Rev. Lett. **91**, 096601 (2003).

[30] N. Marzari, A. A. Mostofi, J. R. Yates, I. Souza, and D. Vanderbilt, *Maximally localized Wannier functions: Theory and applications*, Rev. Mod. Phys. **84**, 1419 (2012).

[31] B. Kramer and A. MacKinnon, *Localization: Theory and experiment*, Rep. Prog. Phys. **56**, 1469 (1993).

[32] P. Lloyd, *Exactly solvable model of electronic states in a three-dimensional disordered Hamiltonian: Non-existence of localized states*, J. Phys. C: Solid State Phys. **2**, 1717 (1969).

[33] D. J. Thouless, *A relation between the density of states and range of localization for one dimensional random systems*, J. Phys. C: Solid State Phys. **5**, 77 (1972).

[34] K. Ishii, *Localization of eigenstates and transport phenomena in the one-dimensional disordered system*, Supp. Prog. Theor. Phys. **53**, 77 (1973).

[35] B. Derrida and E. Gardner, *Lyapounov exponent of the one dimensional Anderson model: Weak disorder expansions*, J. Phys. (Paris) **45**, 1283 (1984).

[36] L. Martin, G. Di Giuseppe, A. Perez-Leija, R. Keil,

F. Dreisow, M. Heinrich, S. Nolte, A. Szameit, A. F. Abouraddy, D. N. Christodoulides, and B. E. A. Saleh, *Anderson localization in optical waveguide arrays with off-diagonal coupling disorder*, Opt. Express. **19**, 13636 (2011).

[37] J. B. Pendry, *Off-diagonal disorder and 1D localisation*, J. Phys. C: Solid State Phys. **15**, 5773 (1982).

[38] M. Inui, S. A. Trugman, and E. Abrahams, *Unusual properties of midband states in systems with off-diagonal disorder*, Phys. Rev. B **49**, 3190 (1994).

[39] T. A. L. Ziman, *Localization with off-diagonal disorder: A qualitative theory*, Phys. Rev. B **26**, 7066 (1982).

[40] J. D. Bodyfelt, D. Leykam, C. Danieli, X. Yu, and S. Flach, *Flatbands under correlated perturbations*, Phys. Rev. Lett. **113**, 236403 (2014).

[41] M. Titov and H. Schomerus, *Anomalous wave function statistics on a one-dimensional lattice with power-law disorder*, Phys. Rev. Lett. **91**, 176601 (2003).

[42] I. Goldhirsch, S. H. Noskowicz, and Z. Schuss, *Spectral degeneracy in the one-dimensional Anderson problem: A uniform expansion in the energy band*, Phys. Rev. B **49**, 14504 (1994).

[43] S. D. Huber and E. Altman, *Bose condensation in flat bands*, Phys. Rev. B **82**, 184502 (2010).

[44] R. A. Vicencio and M. Johansson, *Discrete flat-band solions in the kagome lattice*, Phys. Rev. A **87**, 061803(R) (2013).

[45] M. Johansson, U. Naether, and R. A. Vicencio, *Compactification tuning for nonlinear localized modes in sawtooth lattices*, Phys. Rev. E **92**, 032912 (2015).

[46] L. Ge, *Parity time symmetry in a flat band system*, Phys. Rev. A **92**, 052103 (2015).

[47] V. Dwivedi and V. Chua, *Of bulk and boundaries: Generalized transfer matrices for tight-binding models*, arXiv:1510.04279.